

Interface roughness scattering in ultra-thin N-polar GaN quantum well channels

Uttam Singiseti, Man Hoi Wong, and Umesh K. Mishra

Citation: *Appl. Phys. Lett.* **101**, 012101 (2012); doi: 10.1063/1.4732795

View online: <http://dx.doi.org/10.1063/1.4732795>

View Table of Contents: <http://apl.aip.org/resource/1/APPLAB/v101/i1>

Published by the [American Institute of Physics](http://www.aip.org).

Related Articles

Self-compensation in highly n-type InN
Appl. Phys. Lett. **101**, 011903 (2012)

Intrinsic and extrinsic defect relaxation behavior of ZnO ceramics
J. Appl. Phys. **111**, 124106 (2012)

Carrier transport mechanism of poly(3,4-ethylenedioxythiophene) doped with poly(4-styrenesulfonate) films by incorporating ZnO nanoparticles
APL: Org. Electron. Photonics **5**, 129 (2012)

Carrier transport mechanism of poly(3,4-ethylenedioxythiophene) doped with poly(4-styrenesulfonate) films by incorporating ZnO nanoparticles
Appl. Phys. Lett. **100**, 253302 (2012)

First principles calculation of the electronic properties and lattice dynamics of $\text{Cu}_2\text{ZnSn}(\text{S}_{1-x}\text{Se}_x)_4$
J. Appl. Phys. **111**, 123704 (2012)

Additional information on *Appl. Phys. Lett.*

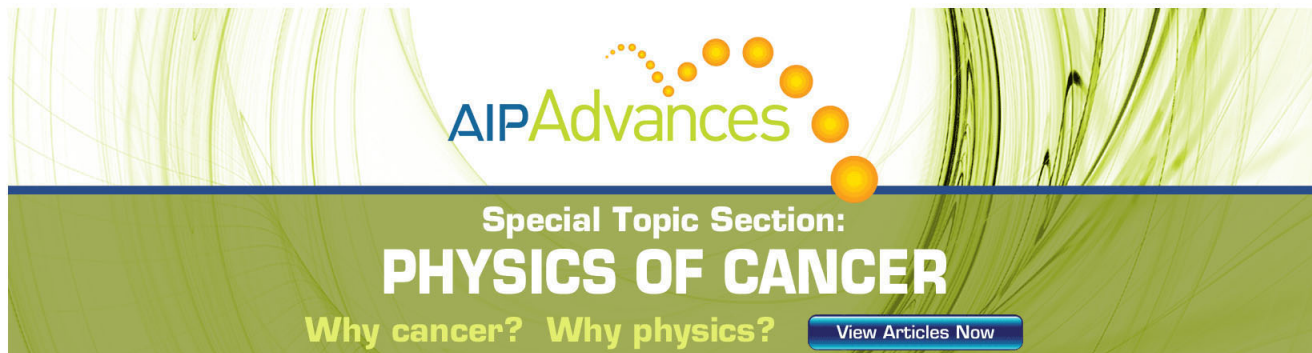
Journal Homepage: <http://apl.aip.org/>

Journal Information: http://apl.aip.org/about/about_the_journal

Top downloads: http://apl.aip.org/features/most_downloaded

Information for Authors: <http://apl.aip.org/authors>

ADVERTISEMENT

The advertisement features a green and white background with a pattern of thin, curved lines. At the top, the 'AIP Advances' logo is displayed in green and blue. Below it, the text 'Special Topic Section: PHYSICS OF CANCER' is written in white on a dark green background. At the bottom, the phrase 'Why cancer? Why physics?' is written in white, followed by a blue button with the text 'View Articles Now' in white.

AIP Advances

Special Topic Section:
PHYSICS OF CANCER

Why cancer? Why physics? [View Articles Now](#)

Interface roughness scattering in ultra-thin N-polar GaN quantum well channels

Uttam Singiseti,^{1,a)} Man Hoi Wong,² and Umesh K. Mishra³

¹Electrical Engineering Department, University at Buffalo, Buffalo, New York 14260, USA

²SEMATECH Inc., Austin, Texas 78741, USA

³ECE Department, University of California, Santa Barbara, California 93106, USA

(Received 8 May 2012; accepted 16 June 2012; published online 2 July 2012)

In this Letter, we report experimental and theoretical investigations on the effect of the channel thickness on the low-field electron mobility in N-polar GaN quantum well channels. From temperature dependent Hall mobility data and numerical modeling of the mobility, the interface roughness is identified as a strong factor in determining the low field mobility as the channel thickness is scaled down. In the graded AlGaIn back-barrier N-polar GaN field effect transistor structures studied here, the roughness leads to localization of electrons at a channel thickness of 3.5 nm leading to extremely low mobility. © 2012 American Institute of Physics. [<http://dx.doi.org/10.1063/1.4732795>]

High frequency GaN field effect transistors (FETs) have made rapid progress in recent years by aggressive gate length scaling to 20 nm with a peak current gain cutoff frequency (f_t) of 343 GHz.¹ Along with decreasing gate lengths, the vertical dimension of the device such as the gate barrier thickness and channel thickness needs to be scaled in order to maintain the electrostatic integrity of the FET. InGaIn back-barrier, AlGaIn buffer layers, and GaN quantum well channels have been used to increase carrier confinement in these scaled devices.^{2–4} N-polar GaN FETs with a top gate dielectric and a bottom charge inducing wide bandgap AlGaIn back-barrier provide a structure similar to ultrathin body silicon-on-insulator (UTB-SOI) devices and hence have the potential advantage in scaling to sub-50 nm gate lengths.⁵

Recently, self-aligned N-polar GaN devices have been demonstrated with high frequency operation^{6–8} and also with low source access resistances (R_s) obtained by source/drain regrowth. As the N-polar GaN devices are scaled vertically (gate dielectric thickness and channel thickness) along with lateral scaling of gate length to sub-50 nm dimensions, the low field electron mobility in the channel is affected. The mobility in these vertically scaled channels needs to be high in order to maintain high ballisticity⁹ and low parasitic access resistance, which are critical to improve high frequency performance. The reported two-dimensional electron gas (2-DEG) mobilities in N-polar devices have a large variation with peak reported mobility of 1700 cm²/V s for 15 nm thick channels¹⁰ and a low mobility of 350 cm²/V s in an 8 nm thick channel.¹¹ A number of theoretical and experimental investigations of the electron mobility in N-polar devices have been reported.^{12–14} However, there has been no theoretical study reported on the impact of the channel thickness and the effect of roughness scattering on the low field mobility of N-polar devices. Unlike the conventional Ga-polar AlGaIn/GaN high electron mobility transistors

(HEMTs), the channel in the N-polar device is a double hetero-structure quantum well (Fig. 1), which gives rise to additional scattering mechanisms that affect the low-field electron mobility. In this Letter, we report both a theoretical and an experimental investigation on the impact of the channel thickness on the electron mobility in N-polar quantum well channels. Roughness scattering, charged dislocation scattering, acoustic phonon (AP) scattering, and remote impurity scattering have been included in the mobility model providing extra insight into the mobility limiting mechanisms.

Fig. 1 shows the band diagram of the sidewall access region of a self-aligned N-polar FET with a 5 nm GaN channel.^{6,11} The conductivity of this un-gated sidewall access region, determined by the 2-DEG density and the mobility, is critical in these devices to reduce the source access resistance (R_s). For our investigation into mobility limiting mechanisms in thin quantum well structures, we study the mobility of this structure. Four samples with channel thicknesses of 12 nm, 8 nm, 5 nm, and 3.5 nm were investigated here; all of them have the same layer structure shown in Fig. 1(a) except for the channel thickness. They were grown within a short period of time to minimize any drift in the device material quality. The devices were grown by plasma-assisted molecular beam epitaxy (PA-MBE) on C-face SiC with an insulating buffer. The device structure consisted of a top GaN channel, a 2 nm AlN back-barrier, a 5 nm unintentionally doped Al_{0.25}Ga_{0.75}N setback layer, a 30 nm graded AlGaIn modulation doping layer ([Si] = 4.5×10^{18} cm⁻³), and a GaN buffer. The AlN interlayer between the GaN channel and AlGaIn barrier was introduced to reduce the alloy scattering.¹³ The graded AlGaIn barrier with Si modulation doping was used to reduce high frequency current collapse and the output conductance in the devices.¹⁵ After the growth, the devices were diced into 7 mm × 7 mm square pieces for Hall measurement in Van der Pauw geometry. Next, the surface oxide was removed with 1 min buffered hydro-fluoric acid (BHF) treatment before deposition of 50 nm of silicon nitride (SiN_x) by plasma-enhanced chemical

^{a)}Email: uttamsin@buffalo.edu. Telephone: (716) 645-1536. Fax: (716) 645-3656.

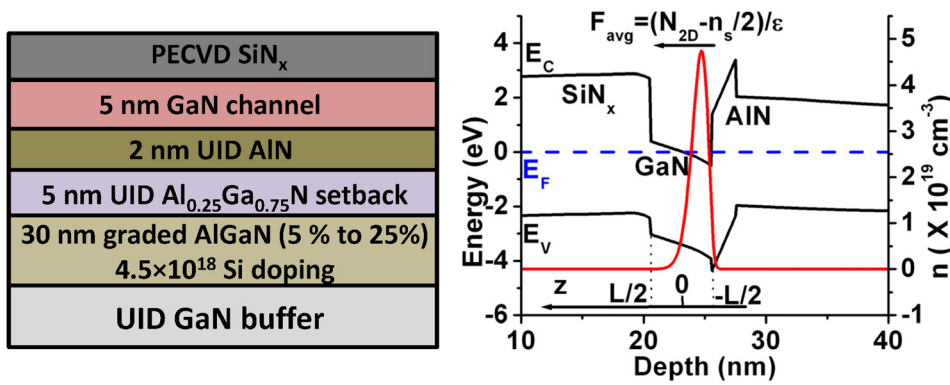


FIG. 1. (a) The layer structure schematic and (b) simulated band diagram and electron density of the 5 nm GaN channel device. The UID in the AlN inter layer is $1 \times 10^{18} \text{ cm}^{-3}$, the doping in the AlGa_N graded layer is $4.5 \times 10^{18} \text{ cm}^{-3}$.

vapor deposition (PECVD). Annealed indium contacts were formed at the corners of the square pieces for Hall measurement.

The measured 2-DEG density and Hall mobility at room temperature (RT) for the samples are shown in Fig. 2. Both the 2-DEG density and the Hall mobility show a continuous decrease with channel thickness with an extremely low mobility of $65 \text{ cm}^2/\text{V s}$ for the 3.5 nm channel. The decrease in the 2-DEG density is expected due to the Fermi-level pinning at the SiN_x/GaN interface,¹⁶ which depletes electrons as the channel thickness is reduced. To understand the mechanism limiting the mobility in thin channels, temperature dependent Hall mobility was measured for all the samples. Fig. 3 shows the measured Hall mobility for all the samples from 15 K to room-temperature (300 K).

We observed two distinctly different trends of mobility with temperature. The mobility variation of the 12 nm, 8 nm, and 5 nm samples show similar behavior of increasing mobility with decreasing temperature and then saturation, while the 3.5 nm channel device shows decreasing mobility with decreasing temperature. For the 12 nm, 8 nm, and 5 nm samples, the mobility first increased with decreasing temperature as expected due to the reduction of optical phonon (OP) and acoustic phonon scattering rates. However, the mobility saturated at a relatively lower value of $<2000 \text{ cm}^2/\text{V s}$ as com-

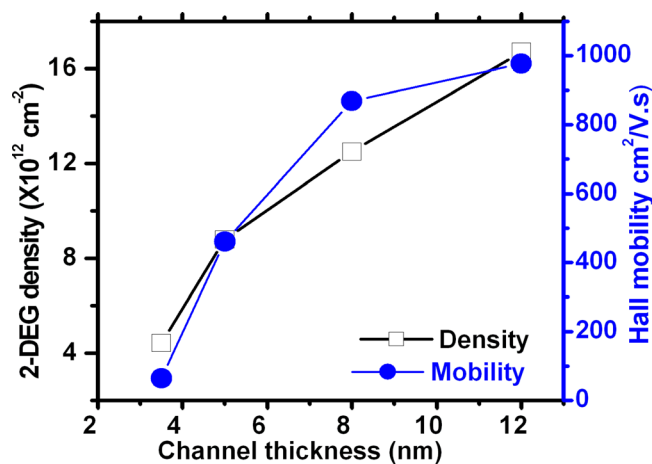


FIG. 2. Measured room temperature Hall mobility and 2-DEG density as a function of GaN channel thickness.

pared to Ga-polar GaN HEMTs. The saturation of mobility at lower values suggests a temperature independent Coulombic scattering mechanism as the limiting scattering phenomenon in these devices.

To further understand the phenomenon, we calculated the 2-DEG mobility in the relaxation time approximation and in the electric quantum limit of ground state sub-band occupancy. We have included the interface roughness (IR) scattering in the calculations of mobility in N-polar GaN quantum well channels. The IR scattering has been shown to be important in thin quantum well structures.¹⁷ The other scattering mechanisms included are OP scattering, AP scattering, ionized impurity scattering (II), scattering due to charged dislocations, scattering due to un-intentional doping (UID) in the AlN interlayer, and scattering due to trapped charges in the PECVD SiN_x.

The roughness scattering calculation in GaAs quantum wells¹⁷ assumed a symmetric quantum well; however the quantum well channels studied here have a high electric field in the channel arising from the polarization in the wurtzite III-N system. Recently, roughness scattering calculation was reported for GaAs quantum wells with an electric field using 2nd order perturbation theory.¹⁸ However, the perturbation

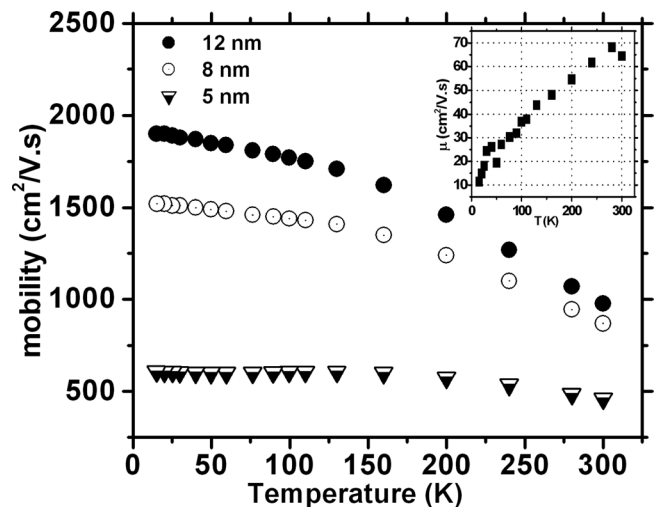


FIG. 3. Measured Hall mobility as a function of temperature for the 12 nm, 8 nm, and 5 nm channels. The inset shows the measured Hall mobility for the 3.5 nm channel device.

theory cannot be applied for the N-polar GaN channels because of the high magnitude of the electric fields (\sim MV/cm). Instead, for an electron confined in a quantum well with a positive electric field (F) in the direction of growth (z -axis in Fig. 1), we use a variational wave function which is given by^{19,20}

$$\psi(z) = N(\beta)\cos\left(\frac{\pi z}{L}\right)\exp\left(-\beta\left(\frac{z}{L} + \frac{1}{2}\right)\right), \quad |z| < L/2, \quad (1)$$

where L is the channel thickness, $N^2(\beta) = 4\beta(\beta^2 + \pi^2)\exp(2\beta)/L\pi^2(\exp(2\beta) - 1)$ is the normalization constant, and β is the variational parameter that depends on the electric field (F) in the channel. This form of wave functions has been reported to predict the correct energy Eigen states for high electric fields.^{19,20} The ground state energy for this variational wave function is given by¹⁹

$$E_1 = \frac{\hbar^2\pi^2}{2m^*L^2} - \frac{1}{2}eFL + \left(\frac{3}{2}\right)^{5/3}\left(\frac{e^2F^2\hbar^2}{m^*}\right)^{1/3}, \quad (2)$$

With $\beta_{\min} = ((3/4)\pi^2 eFL/(\hbar^2\pi^2/2m^*L^2))^{1/3}$ when the electric field (F) in the channel is large. The scattering potential due to thickness fluctuations in the quantum well thickness can be calculated similar to the approach in Ref. 17 by

$$\delta E_1 = \frac{\partial E_1}{\partial L}\Delta(r) = -\left(\frac{eF}{2} + \frac{\hbar^2\pi^2}{m^*L^3}\right)\Delta(r), \quad (3)$$

where r is the in-plane vector, and the square of the scattering Hamiltonian is given by

$$H_{IR}^2 = \left(\frac{eF}{2} + \frac{\hbar^2\pi^2}{m^*L^3}\right)^2 \pi\Delta^2\Lambda^2\exp\left(-\frac{\Lambda^2q^2}{4}\right), \quad (4)$$

where Δ and Λ are the quantum well thickness fluctuation height and correlation length parameters with a Gaussian auto-correlation function,¹⁷ $q = |\mathbf{k}-\mathbf{k}'| = 2k\sin(\theta/2)$, and \mathbf{k} and \mathbf{k}' are the initial and final the wave vector of the electron.¹⁸ The first term of this Hamiltonian is similar to the traditional roughness scattering at the Si/SiO₂ interface in bulk Si MOSFETs with F^2 electric field dependence and the second term is the quantum well thickness fluctuations that is dominant in thin channels with $1/L^6$ dependence as reported

in Ref. 17. Finally, the scattering rate due to roughness is calculated by Fermi's Golden rule including screening as

$$\frac{1}{\tau_{IR}} = \frac{2\Delta^2\Lambda^2m^*}{\hbar^3}\left(\frac{eF}{2} + \frac{\hbar^2\pi^2}{m^*L^3}\right)^2 \int_0^1 \frac{u^4\exp(-u^2\Lambda^2k_F^2)}{\left(u + G(q)\frac{qTF}{2k_F}\right)^2\sqrt{1-u^2}}du, \quad (5)$$

where k_F is the Fermi wave vector, $u = q/k_F$, q_{TF} is the Thomas-Fermi screening vector, and $G(q)$ is the form factor for screening due to the finite width of the 2-DEG. We use Price's approximation²¹ for $G(q)$ which is given by $G(q) \cong 1/(1+bq)$ where $b = (\int 2\psi^2 dz)^{-1}$.

For the other Columbic scattering mechanisms (charged dislocation scattering, ionized impurity, trapped charge in the SiN dielectric), a form factor $F(q)$ due to the finite width of 2-DEG wave function is used $F(q) = \int_{-\infty}^{+\infty} \psi^2(z)\exp[q|z-d|]dz$, where d is the distance of the delta doping from the 2-DEG. The alloy scattering is negligible in these devices because the 2 nm thick AlN interlayer with a large conduction band offset with GaN quenches the wavefunction rapidly with an extremely low probability of the wavefunction in the AlGaIn alloy layer. For a comparison with the other scattering mechanisms, alloy scattering calculations were done with a modified Fang-Howard wave function and found to be negligible compared to the other mechanisms considered here.

The final scattering rates of the different scattering mechanisms affecting mobility were calculated numerically in MATLAB for a temperature range of 15 K to RT, and Matthiessen's rule was used to calculate the total mobility. For the variational waveform calculation, the electric field in the channel was taken as the average electric field given by $F_{avg} = e(N_{2D} - n_s/2)/\epsilon_{GaIn}$, where n_s is the measured 2-DEG density and N_{2D} is the total 2-D doping density.

Fig. 4 shows the measured and calculated mobility for the 5 nm, 8 nm, and 12 nm GaN channels. The roughness parameters of $\Delta = 0.48$ nm and $\Lambda = 3.0$ nm were used to fit the low temperature mobility of the 8 nm channel. The same Δ and Λ values are used for calculating the mobility for the 12 nm, 5 nm, and 3 nm samples. The Δ value is larger than

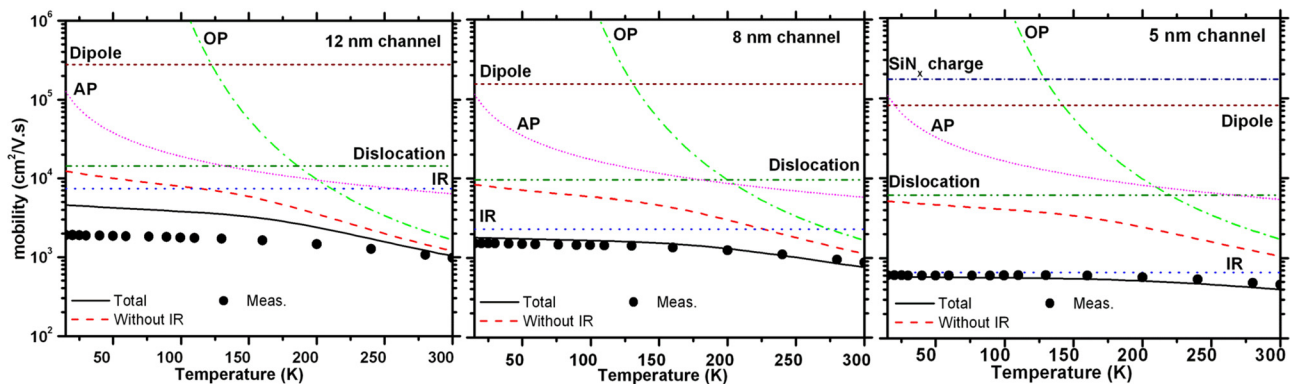


FIG. 4. Calculated and measured mobilities for the 12 nm, 8 nm, and 5 nm channel device. The dislocation density is assumed to be $1 \times 10^{10} \text{ cm}^{-2}$ with a filling factor $f = 0.5$, the trapped charge in the SiN_x is assumed to be $1 \times 10^{13} \text{ cm}^{-2}$, the optical phonon energy for GaN is 92 meV and the deformation potential for acoustic phonons is 9.1 eV. For IR scattering, $\Delta = 0.48$ nm and $\Lambda = 3.0$ nm are used for all the samples. The roughness parameters of the top and bottom interfaces are assumed to be same and uncorrelated. The F_{avg} for 12 nm, 8 nm, 5 nm, and 3.5 nm samples are 1.25 MV/cm, 1.67 MV/cm, 2.0 MV/cm, and 2.34 MV/cm, respectively.

the typical values in Ga-polar GaN HEMTs.²² The inverted N-polar HEMT structure where the GaN channel is grown on an AlN layer with an underlying Si doping layer could be the reason for larger value similar to the higher roughness observed in inverted AlGaAs/GaAs HEMTs. The atomic force microscopy (AFM) root mean square (rms) surface roughness (not shown) of the wafers grown under similar conditions with a similar layer structure was 0.6-0.8 nm, which is again higher than typical Ga-polar GaN HEMTs.

As seen in Fig. 4, the mobility due to roughness scattering (labeled IR in Fig. 4) with same Δ and Λ values increases rapidly as the GaN channel thickness is reduced from 12 nm to 5 nm. Both components of the roughness scattering increase with decreasing thickness (Eq. (4)). As the channel thickness was reduced, the 2-DEG density (n_s) in the channel decreases due to the depletion from the surface pinning at the SiN_x/GaN interface, which results in an increase in the average field in the channel ($F_{avg} = e(N_{2D} - n_s/2)/\epsilon_{GaN}$) as N_{2D} is same for all samples. The increased field subsequently leads to higher roughness scattering due to the F^2 dependence (Eq. (4)). The second component of roughness scattering also increases rapidly for channel thickness of 5 nm due to the $1/L^6$ dependence (Eq. (4)). The decreased n_s in thin channels also leads to decreased k_F , which increases the integral in Eq. (5). The figure also shows the total calculated mobility without roughness scattering, which clearly predicts very high mobility values compared to the measured values. The discrepancy between the calculated and measured low temperature mobility of the 12 nm sample could be due to the non-inclusion of the 2nd sub-band occupation in the mobility calculations, which is highly likely due to the large 2-DEG density of $1.7 \times 10^{13} \text{ cm}^{-2}$.

The calculated mobility for the 3.5 nm channel device with $4 \times 10^{12} \text{ cm}^{-2}$ 2-DEG density and the same roughness parameters is $100 \text{ cm}^2/\text{V s}$ while the measured value is $65 \text{ cm}^2/\text{V s}$. The discrepancy can be understood from the temperature dependent mobility. Unlike the other samples, the measured mobility for the 3.5 nm device decreases with temperature, while the model predicts (not shown) a constant mobility of $100 \text{ cm}^2/\text{V s}$ with decreasing temperature. This observed trend of mobility with temperature can be explained by strong localization of electrons in the channel due to the high roughness. The localization leads to hopping type conduction, which is a thermally activated process and hence the mobility decreases with decreasing temperature. This further validates that the roughness is an issue in the structures studied here. Current transport theory in disordered systems and metal insulator transition (MIT) theory can be applied to understand the mobility versus temperature data for the 3.5 nm sample.²³ It is noted that the 2-DEG density remained unchanged from 15 K to RT in all the samples. From the expression for the roughness scattering, it is clear that the mobility can be increased by decreasing the electric field in the channel and having smoother interfaces. The calculated RT mobility for the 3.5 nm GaN channel device with $1 \times 10^{13} \text{ cm}^{-2}$ 2-DEG density (i.e., reduced depletion from the SiN_x/GaN interface states) and $\Delta = 0.25 \text{ nm}$ is $824 \text{ cm}^2/\text{V s}$ and it is $1250 \text{ cm}^2/\text{V s}$ with $\Delta = 0.1 \text{ nm}$, which are reason-

ably high values for the ultra-thin quantum well channel FETs.

In conclusion, we have studied the dependence of mobility in N-polar GaN quantum well channels with thickness. We have incorporated roughness scattering for N-polar GaN quantum well channel mobility calculation and shown that it is the principle reason for lower mobility in the thin channels. Furthermore, the roughness leads to hopping conduction in 3.5 nm channels. Future work correlating roughness and mobility to the device structure, growth method, and growth conditions will be important in scaling the channel thickness for high frequency devices.

This work was supported by the DARPA NeXT program. A portion of this work was performed in the UCSB nanofabrication facility, part of the NSF funded NNIN network. The authors would like to thank Nik Toledo for dicing the samples into square pieces and Jim Speck for carefully reading the manuscript.

- ¹K. Shinohara, D. Regan, A. Corrion, D. Brown, S. Burnham, P. J. Willadsen, I. Alvarado-Rodriguez, M. Cunningham, C. Butler, A. Schmitz, S. Kim, B. Holden, D. Chang, V. Lee, A. Ohoka, P. M. Asbeck, and M. Micovic, in *2011 IEEE International Electron Devices Meeting (IEDM)* (2011), pp. 19.11.11–19.11.14.
- ²D. S. Lee, L. Bin, M. Azize, G. Xiang, G. Shiping, D. Kopp, P. Fay, and T. Palacios, in *2011 IEEE International Electron Devices Meeting (IEDM)* (2011), pp. 19.12.11–19.12.14.
- ³D. S. Lee, G. Xiang, G. Shiping, and T. Palacios, *IEEE Electron Device Lett.* **32**(5), 617–619 (2011).
- ⁴G. Li, R. Wang, J. Guo, J. Verma, Z. Hu, Y. Yue, F. Faria, Y. Cao, M. Kelly, T. Kosel, H. Xing, and D. Jena, *IEEE Electron Device Lett.* **33**(5), 661–663 (2012).
- ⁵D. Guerra, M. Saraniti, N. Faralli, D. K. Ferry, S. M. Goodnick, and F. A. Marino, *IEEE Trans. Electron Devices* **57**(12), 3348–3354 (2010).
- ⁶U. Singiseti, M. H. Wong, J. S. Speck, and U. K. Mishra, *IEEE Electron Device Lett.* **33**(1), 26–28 (2012).
- ⁷Nidhi, S. Dasgupta, D. F. Brown, J. S. Speck and U. K. Mishra, in *2011 69th Annual Device Research Conference (DRC)* (2011), pp. 141–142.
- ⁸Nidhi, S. Dasgupta, J. Lu, F. Wu, S. Keller, J. S. Speck and U. K. Mishra, in *2011 69th Annual Device Research Conference (DRC)* (2011), pp. 279–280.
- ⁹M. S. Lundstrom, *IEEE Electron Device Lett.* **22**(6), 293–295 (2001).
- ¹⁰M. H. Wong, S. Rajan, R. M. Chu, T. Palacios, C. S. Suh, L. S. McCarthy, S. Keller, J. S. Speck, and U. K. Mishra, *Phys. Status Solidi A* **204**(6), 2049–2053 (2007).
- ¹¹U. Singiseti, M. H. Wong, S. Dasgupta, J. S. Speck, and U. K. Mishra, *Appl. Phys. Express* **4**, 024103 (2011).
- ¹²D. F. Brown, S. Rajan, S. Keller, Y.-H. Hsieh, S. P. DenBaars, and U. K. Mishra, *Appl. Phys. Lett.* **93**(4), 042104–042103 (2008).
- ¹³S. Kolluri, S. Keller, D. Brown, G. Gupta, S. Rajan, S. P. DenBaars, and U. K. Mishra, *J. Appl. Phys.* **108**(7), 074502–074504 (2010).
- ¹⁴Nidhi, O. Bierwagen, S. Dasgupta, D. F. Brown, S. Keller, J. S. Speck, and U. K. Mishra, in *2010 Electronic Materials Conference (EMC)*, South Bend, IN (2010).
- ¹⁵M. H. Wong, U. Singiseti, J. Lu, J. S. Speck, and U. K. Mishra, in *2011 69th Annual Device Research Conference (DRC)* (2011), pp. 211–212.
- ¹⁶Nidhi, S. Rajan, S. Keller, F. Wu, S. P. DenBaars, J. S. Speck, and U. K. Mishra, *J. Appl. Phys.* **103**(12), 124508–124504 (2008).
- ¹⁷H. Sakaki, T. Noda, K. Hirakawa, M. Tanaka, and T. Matsusue, *Appl. Phys. Lett.* **51**(23), 1934–1936 (1987).
- ¹⁸R. K. Jana and D. Jena, *Appl. Phys. Lett.* **99**(1), 012104–012103 (2011).
- ¹⁹D. Ahn and S. L. Chuang, *Appl. Phys. Lett.* **49**(21), 1450–1452 (1986).
- ²⁰D. A. B. Miller, D. S. Chemla, T. C. Damen, A. C. Gossard, W. Wiegmann, T. H. Wood, and C. A. Burrus, *Phys. Rev. B* **32**(2), 1043–1060 (1985).
- ²¹P. J. Price, *J. Vac. Sci. Technol.* **19**(3), 599–603 (1981).
- ²²Y. Cao and D. Jena, *Appl. Phys. Lett.* **90**(18), 182112 (2007).
- ²³A. Gold and W. Götze, *Phys. Rev. B* **33**(4), 2495–2511 (1986).